

## Acoustic-phonon transmission in quasiperiodic superlattices

S. Tamura\* and J. P. Wolfe

Department of Physics and Materials Research Laboratory, University of Illinois at Urbana-Champaign,  
Urbana, Illinois 61801

(Received 9 June 1987)

Acoustic-phonon transmission through a realistic Fibonacci superlattice is studied theoretically. We find a number of transmission dips corresponding to Bragg-like reflections of phonons. The transmission spectrum is much more complex than in the periodic case; however, the strongest dips in transmission are remarkably correlated with those of the periodic superlattice. We also present the first realistic calculations of the phonon dispersion relations in an actual quasiperiodic superlattice. For oblique angles of incidence, intermode Bragg-like reflections of the phonons are predicted.

Since the discovery<sup>1</sup> of quasicrystalline phases in metallic alloys there has been a number of studies<sup>2-4</sup> on the vibrational properties of one-dimensional (1D) quasiperiodic systems. Recently, Merlin *et al.*<sup>5</sup> have fabricated semiconductor superlattices in a 1D quasiperiodic fashion. Basically, two different building blocks *A* and *B* of GaAs/AlAs are layered according to a well-prescribed rule, such that the ratio of these *A* and *B* blocks equals the golden mean,  $\tau = (1 + \sqrt{5})/2$ . The prescribed sequence of blocks, *ABAABABA* . . . , produces a "Fibonacci superlattice." X-ray and Raman scattering measurements<sup>5-7</sup> have revealed the special characteristics of this nonperiodic heterostructure.

We shall study here the acoustic phonon transmission in a Fibonacci superlattice. In a periodic superlattice with periodicity  $\tilde{d}$  the phonons satisfying the condition  $q = q_n \equiv n\pi/\tilde{d}$  are Bragg reflected, where  $q$  is the normal component of the wave vector and  $n$  is an integer specifying the order of the Bragg reflection. This means that phonons with  $q = q_n$  cannot propagate through an ideal superlattice with an infinite number of periods, and frequency gaps are created at  $q = q_n$ . For a superlattice with a finite number of periods, the exact periodicity is lost, but there are distinct dips in the transmission for phonons with frequencies in the band gaps. These dips in transmission have been observed both by phonon spectroscopy<sup>8,9</sup> and by phonon imaging.<sup>10</sup>

In a superlattice, the interference effects between the incident and reflected phonons are described by the structure factor

$$S_Q = \sum_j \exp(iQz_j), \quad (1)$$

where  $Q$  is the sum of the normal components of the wave vectors of the incident and reflected phonons. For instance,  $Q = 2q$  for a reflection in which the mode of the phonon does not change. In this equation  $\{z_j\}$  defines the positions of the interfaces. The structure factor for a periodic system is simply  $S_Q = (2\pi/\tilde{d}) \sum_n \delta(Q - 2q_n)$ . Calculations of the structure factor for quasiperiodic systems have been made via direct<sup>11</sup> and projection methods.<sup>12</sup> The result for the Fibonacci superlattice consisting of *A* and *B* layers with thickness  $d_A$  and  $d_B$  and for

$d_A/d_B = \tau$  (which is approximately satisfied by the sample<sup>5</sup>) is

$$S_Q \propto \sum_{m,n} \frac{\sin X_{m,n}}{X_{m,n}} \exp(iX_{m,n}) \delta(Q - Q_{m,n}), \quad (2)$$

where  $X_{m,n} = \pi\tau(m\tau - n)/(1 + \tau^2)$ ,  $Q_{m,n} = 2\pi(m + n\tau)/d$ , and  $d = \tau d_A + d_B$ . Thus, the constructive interference between the incident and reflected phonons of definite polarization occurs for  $q = q_{m,n} \equiv Q_{m,n}/2$ , which leads to dips in transmission for phonons of frequencies  $\nu = \nu_{m,n} \equiv v(m + n\tau)/2d$ , where  $v$  is the relevant sound velocity in the Fibonacci superlattice. The form of the prefactor to the  $\delta$  function in Eq. (2) dictates that the most significant dips in transmission occur for those  $q = q_{m,n}$  for which  $n/m$  is close to  $\tau$ , i.e.,  $m$  and  $n$  are successive Fibonacci numbers,  $(m, n) = (F_{p-1}, F_p)$ , where  $F_{p+1} = F_p + F_{p-1}$  and  $(F_0, F_1) = (0, 1)$ . For these values of  $(m, n)$ ,  $q_{m,n}$  takes the form of (integer)  $\times \pi\tau/d$ . The "order" of the major reflections, therefore, is classified by a single integer  $p$ , and these reflections are commonly labeled  $\tau^p$ .

The phonon transmission rate is calculated by using the transfer matrix for the acoustic fields. As an example we assume the Fibonacci superlattice used in the experiment by Merlin *et al.*<sup>5</sup> in which two building blocks *A* = (42-Å GaAs) (17-Å AlAs) and *B* = (20-Å GaAs) (17-Å AlAs) are deposited in a Fibonacci sequence. First, we consider the case of phonons propagating perpendicular to the interfaces. Let us introduce the two-component vector **U**, consisting of the nonvanishing components of the displacement and stress fields in the superlattice. After propagating through an *A* block, **U** changes to  $T_A \mathbf{U}$ . Here,  $T_A = t_A^{(\text{GaAs})} \times t_A^{(\text{AlAs})}$ , where  $t_A^{(M)}$  is defined by

$$t_A^{(M)} = \begin{pmatrix} \cos \alpha_A^{(M)} & (\beta_A^{(M)})^{-1} \sin \alpha_A^{(M)} \\ -\beta_A^{(M)} \sin \alpha_A^{(M)} & \cos \alpha_A^{(M)} \end{pmatrix}, \quad (3)$$

where  $\alpha_A^{(M)} = k_A^{(M)} d_A^{(M)}$ ,  $\beta_A^{(M)} = k_A^{(M)} \mu_A^{(M)}$ , with  $k_A^{(M)}$ ,  $d_A^{(M)}$ , and  $\mu_A^{(M)}$  defined as the phonon wave number,<sup>13</sup> thickness, and appropriate elastic constant of layer *M* in block *A*.  $T_B$  is defined similarly. We envision an experiment where an acoustic wave incident on the superlattice from the substrate with amplitude  $U_0 = U_5$  passes

through the superlattice of length  $z_N$ , and arrives in a "detector layer" with amplitude  $U_{N+1} = U_D$ . Hence, we have

$$U_{N+1}(z_N + \varepsilon) = T_N U_0(0 - \varepsilon), \quad (4)$$

where  $\varepsilon$  is an infinitesimal positive number and the  $N$ th-order transfer matrix  $T_N$  is given by  $T_N = T_A T_B T_A T_A T_B T_A \dots$ , i.e., the product of  $N$ ,  $T_A$  and  $T_B$  matrices forming a Fibonacci sequence. Explicitly,  $U_0$  and  $U_{N+1}$  are given by

$$U_0(0 - \varepsilon) = \begin{pmatrix} a_S^t + a_S^r \\ \beta_S a_S^t - \beta_S a_S^r \end{pmatrix}, \quad (5)$$

where  $a^t$  and  $a^r$  represent the transmission and reflection coefficients, respectively, and  $S$  and  $D$  denote substrate and detector. By setting  $a_D^r = 0$  and  $a_S^t = 1$  and solving Eq. (4), we obtain the amplitude of the transmitted wave in the detector layer and of the reflected wave in the substrate. The phonon transmission rate is then given by  $|a_D^t|^2$ , because we assume perfect acoustic match between substrate and superlattice and between superlattice and detector. Note that  $|a_D^t|^2 + |a_S^r|^2 = 1$ .

In Fig. 1 we have plotted the transmission rate for transverse acoustic (TA) phonons as a function of frequency. The result for longitudinal acoustic (LA) phonons is very similar to Fig. 1; only the scale of the frequency is changed according to  $\nu \rightarrow \nu(v_L/v_T)$ , where  $v_L$  and  $v_T$  are the sound velocities of the LA and TA phonons, respectively. ( $v_L/v_T \sim 1.42$  for [001] propagation.<sup>14</sup>) The seventh generation of the Fibonacci superlattice which

consists of thirteen  $A$  blocks and eight  $B$  blocks is assumed for the numerical calculation. [As the number of generations tends to infinity (number of  $A$  blocks)/(number of  $B$  blocks) =  $\tau$ .] Several frequencies for which dips in transmission are predicted, i.e.,  $\nu = \nu_{m,n} \equiv (m,n)$ , are indicated by arrows in this figure. As expected, the main dips are observed at  $\nu_{m,n}$  for which  $m$  and  $n$  are neighboring Fibonacci numbers, as indicated by  $\tau^p$ .

For comparison, we have also plotted in Fig. 2 the transmission rate of the TA phonons in the *periodic* superlattice consisting of the sequence  $ABABAB \dots$ . The total of 21  $A$  and  $B$  blocks assumed for the numerical calculation is the same as the seventh generation of the Fibonacci superlattice. All these dips in transmission are due to Bragg reflections of phonons in the periodic system, which predicts dips at  $\nu = \nu_n \equiv nc/2d$ , where  $d = d_A + d_B$  is the periodicity and  $c$  is the transverse sound velocity in the periodic superlattice.<sup>15</sup> The frequencies  $\nu_n$  corresponding to  $n$ th-order Bragg reflection are also indicated by arrows in Fig. 2. Surprisingly, all of the main dips in transmission for the Fibonacci superlattice are very close in width, magnitude, and frequency to the periodic Bragg dips. A similar calculation for a randomly generated sequence of  $A$  and  $B$  shows no such correlations with the periodic case. This observation shows that the Fibonacci superlattice is much more closely related to a periodic superlattice than a random one. Clearly, it would be interesting to study such correlations as the rules for constructing a quasiperiodic lattice are changed.

The transmission spectrum of the Fibonacci superlattice can be understood in terms of the phonon dispersion relation. The dispersion relations for phonons in this system are obtained by imposing a Bloch-like boundary condition<sup>16</sup> to the acoustic fields. Here, we assume an infinite repetition of the "unit cell"  $[0, z_N]$  and put

$$U_{N+1}(z_N + \varepsilon) = \exp(iqz_N) U_0(0 - \varepsilon).$$

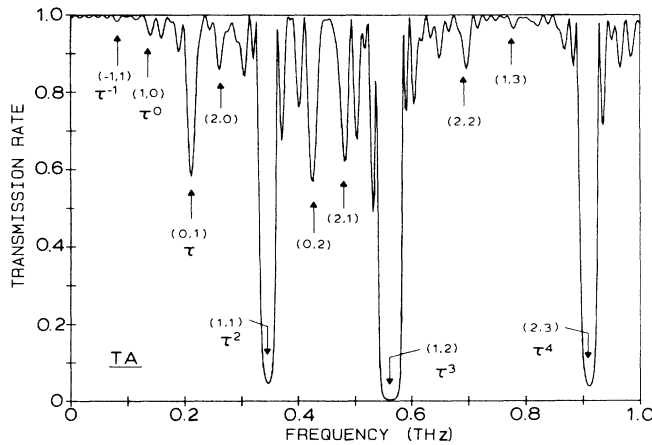


FIG. 1. Frequency dependence of the TA phonon transmission rate in a seven-generation GaAs/AlAs Fibonacci superlattice  $ABAABABAABAABABAABA$ . The propagation direction is perpendicular to the interfaces, i.e., along the [001] direction. Arrows indicate the frequencies  $\nu_{m,n} \equiv (m,n)$ . For those  $m$  and  $n$  that are neighboring Fibonacci numbers  $\nu_{m,n} \sim \tau^p$  and for these frequencies the power of  $\tau$  is explicitly shown.

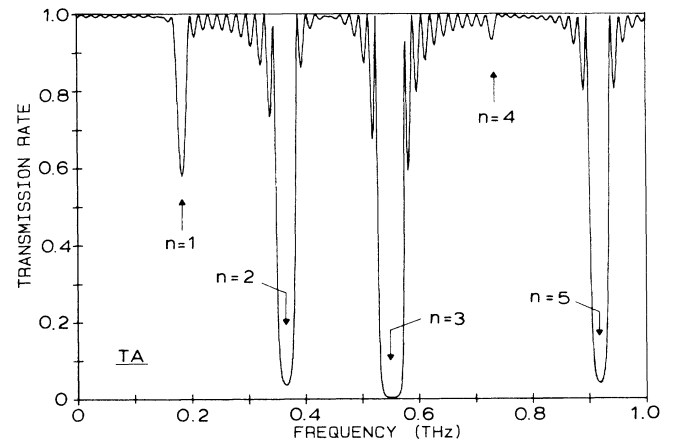


FIG. 2. Frequency dependence of the TA phonon transmission rate in the GaAs/AlAs periodic superlattice consisting of 21  $A$  and  $B$  alternating blocks. Propagation direction is perpendicular to the interfaces. Arrows indicate the frequencies predicted by the Bragg condition, where  $n$  stands for the order of the reflection.

Then, combining with Eq. (4), we find that  $\exp(iqz_N)$  corresponds to the eigenvalue of the transfer matrix  $T_N$ .

Figure 3 shows the dispersion curves of both the TA and LA phonons propagating normal to the Fibonacci superlattice. To our knowledge, these are the first realistic calculations of the phonon dispersion relations in an actual quasiperiodic superlattice. In order to obtain these plots we have divided the frequency range 0 to 1 THz into 2500 intervals and then calculated the wave number for each frequency. Because the wave numbers given by solving the eigenvalue equation are restricted to the values in the interval,  $0 \leq q \leq \pi/z_N$ , we have unfolded this folded zone appropriately to obtain the dispersion relations in the extended zone scheme. Except for the fact that the dispersion curves are almost linear (a consequence of the long wavelength approximation), the results are qualitatively similar to the phonon dispersion relation obtained by Nori and Rodriguez<sup>4</sup> for a nearest-neighbor harmonic chain. That is, many gaps are observed and their structures are almost self-similar. This can be seen for TA phonons in the frequency range 0.2 to 0.6 THz and for LA phonons within 0.3 to 0.8 THz. Specifically, each larger band has two major gaps which split it into three smaller

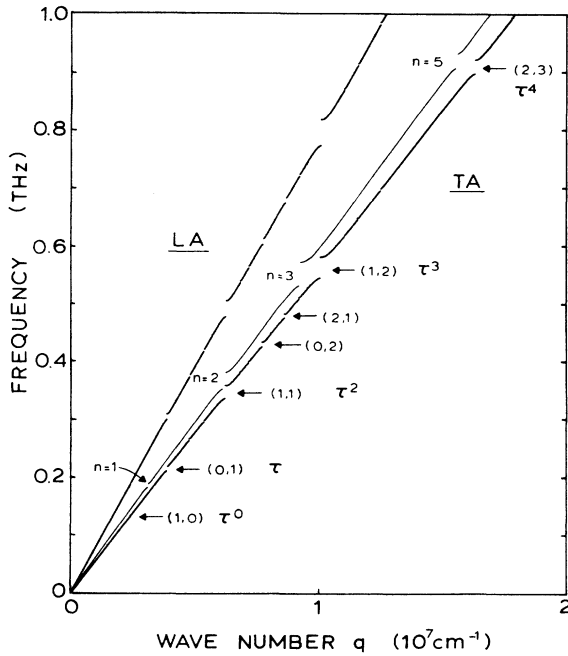


FIG. 3. Dispersion relation of the phonons at normal incidence to a GaAs/AlAs Fibonacci superlattice. Arrows indicate the frequencies  $\nu_{m,n} \equiv (m,n)$ . (See also Fig. 1.) Thin lines show the dispersion relation of the TA phonons in the *periodic* GaAs/AlAs superlattice consisting of alternating *A* and *B* blocks. In order to avoid an overlap of the dispersion curves, we have increased the slope of the “periodic” curve by changing the scale of  $q$  to  $0.95q$ . The correct slope for  $\nu \rightarrow 0$  is  $3.52 \times 10^5$  cm/sec, which is very close to  $3.51 \times 10^5$  cm/sec for the TA mode in the Fibonacci superlattice (Refs. 14 and 15). Gaps in the periodic case are indexed according to the order of the Bragg reflection of the system. The gap corresponding to the fourth-order reflection is too small to be resolved.

bands. In turn, each of the smaller bands has two major gaps, and so on. These band gaps correspond to the frequencies  $\nu_{m,n} \equiv (m,n)$  indicated by arrows in this figure and, likewise, all gaps in the dispersion curves have one-to-one correspondences to the dips in transmission. The dispersion curves plotted in Fig. 3 were computed assuming the ninth Fibonacci generation. For large generation numbers the curves are independent of generation number.

For comparison, we have also plotted in Fig. 3 the dispersion curve of the TA phonons in the periodic superlattice (thin lines). Note that the horizontal scale has been changed from  $q$  to  $0.95q$  for this curve to avoid the overlap of the two dispersion curves. The gaps in the dispersion curve of the periodic lattice are due to Bragg reflections at  $q = q_n$ . Here, we again see that these gaps correlate well with the main gaps of the quasiperiodic system.

So far, we have shown the results for phonons propagating perpendicular to the interfaces. For oblique phonon propagation, the situation becomes much more complicated. Mode conversions occur among the three different polarizations of phonons due to reflections at the interfaces. Consequently,  $\mathbf{U}$  becomes a vector with six elements and the transfer matrix is a  $6 \times 6$  matrix instead of a  $2 \times 2$ . For the periodic case, a remarkable result of the mode conversion is the presence of the intermode Bragg reflections, as recently predicted theoretically<sup>17</sup> and then verified experimentally.<sup>10</sup> Specifically, band gaps appear *inside* the folded zone due to the coupling of TA and LA phonons at oblique propagation directions. A similar effect is also expected for phonons in the quasiperiodic superlattice. Actually, strong intermode phonon reflections in the quasiperiodic system are also predicted by Eq. (2).

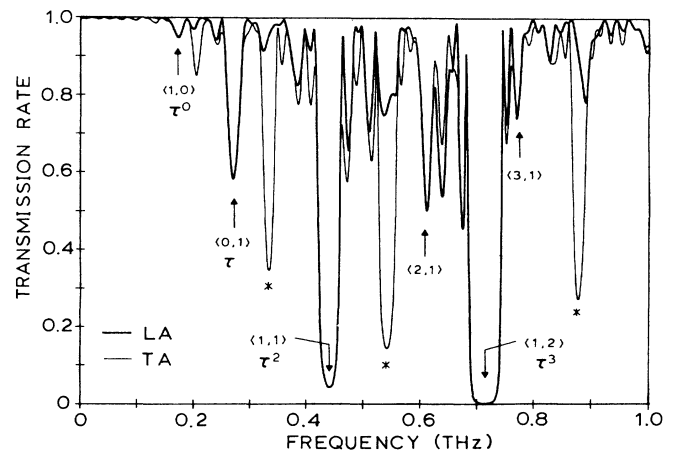


FIG. 4. Transmission rate of phonons propagating in the (110) plane and oblique to the interfaces. Polarization vectors are also in the (110) plane. Angles of incidence of the wave vector are  $17.3^\circ$  for the TA (thin line) and  $30.0^\circ$  for the LA (bold line) phonons in the GaAs layer. (These phonons are excited simultaneously in the superlattices by Snell's law.) Several frequencies  $\nu_{m,n} \equiv (m,n)$  corresponding to intermode Bragg-like reflections are indicated by arrows. Strong dips labeled by \* are due to intramode Bragg-like reflections of TA phonons.

The LA to TA reflection corresponds to  $Q = q_L + q_T$ , where  $q_L$  and  $q_T$  are the normal components of the LA and TA phonons, respectively.<sup>10,17</sup> This condition implies

$$v = \tilde{v}_{m,n} \equiv \left[ \frac{1}{v_L} + \frac{1}{v_T} \right]^{-1} (m + n\tau)/d. \quad (6)$$

In Fig. 4 we have plotted the transmission rates of both TA (thin line) and LA (bold line) phonons propagating in the (110) sagittal plane of the previously described (001)-AlAs/GaAs Fibonacci superlattice.<sup>18</sup> For a wave-vector angle of incidence of 30° for LA phonons in a GaAs layer, the angle of the reflected TA phonons is 17.3° in GaAs, as determined by the conservation of a wave vector parallel to the interface. (Likewise, an incident TA phonon at 17.3° produces a reflected LA phonon at 30°.) Notably, dips labeled by  $\tau^p$  in Fig. 4 are common to both TA and LA phonons. These dips correspond to the intermode phonon reflections in the Fibonacci superlattice. We have indicated by the arrows the frequencies  $\tilde{v}_{m,n} \equiv \langle m, n \rangle$  predicted by Eq. (6).<sup>19</sup> The coincidence of these predicted  $\tilde{v}_{m,n}$  with the locations of the

dips are excellent. Note that there exist strong dips (labeled by \*) which are not common to both modes. Therefore, these dips do not correspond to intermode reflections but rather to intramode Bragg-like reflections of the TA phonons.

To conclude, we have computed the transmission spectrum and dispersion relation of acoustic phonons in a Fibonacci superlattice. The main transmission dips strongly resemble those of a periodic superlattice with the same number and size of unit blocks. This indicates that the Fibonacci lattice is much more closely related to a regular periodic lattice than to a random lattice. As for the periodic case, oblique propagation leads to intermode Bragg-like reflections in the quasiperiodic superlattices.

The authors thank F. Nori for stimulating our interest to this problem. One of us (S.T.) acknowledges a travel grant by the Department of Education, Science, and Culture of Japan. This work was supported by the National Science Foundation under the Materials Research Laboratory Grant No. NSF-DMR-83-16981.

\*Permanent address: Department of Engineering Science, Hokkaido University, Sapporo 060, Japan.

<sup>1</sup>D. Schechtman, I. Blech, D. Gratias, and J. W. Cahn, Phys. Rev. Lett. **53**, 1951 (1984).

<sup>2</sup>J. P. Lu, T. Odagaki, and J. L. Birman, Phys. Rev. B **33**, 4809 (1986).

<sup>3</sup>M. Kohmoto and J. R. Banavar, Phys. Rev. B **34**, 563 (1986).

<sup>4</sup>F. Nori and J. P. Rodriguez, Phys. Rev. B **34**, 2207 (1986).

<sup>5</sup>R. Merlin, K. Bajema, R. Clarke, F. Y. Juang, and P. K. Bhat-tacharya, Phys. Rev. Lett. **55**, 1768 (1985).

<sup>6</sup>J. Todd, R. Merlin, R. Clarke, K. M. Mohanty, and J. D. Axe, Phys. Rev. Lett. **57**, 1157 (1986).

<sup>7</sup>M. W. C. Charma-wardana, A. H. MacDonald, D. J. Lockwood, J. M. Baribeau, and D. C. Houghton, Phys. Rev. Lett. **58**, 1761 (1987).

<sup>8</sup>V. Narayanamurti, H. L. Stormer, M. A. Chin, A. C. Gossard, and W. Wiegmann, Phys. Rev. Lett. **43**, 2012 (1979).

<sup>9</sup>O. Koblinger, J. Mebert, E. Dittrich, S. Dottinger, and W. Eisenmenger, in *Proceedings of the Fifth International Conference of Phonon Scattering in Condensed Matter*, edited by A. C. Anderson and J. P. Wolfe (Springer, New York, 1986), p. 156.

<sup>10</sup>D. C. Hurley, S. Tamura, J. P. Wolfe, and H. Morkoc, Phys. Rev. Lett. **58**, 2446 (1987).

<sup>11</sup>D. Levine and P. J. Steinhardt, Phys. Rev. Lett. **53**, 2477 (1984); Phys. Rev. B **34**, 596 (1986).

<sup>12</sup>R. K. P. Zia and W. J. Dallas, J. Phys. A **18**, L341 (1985).

<sup>13</sup>Note that the wave number  $k_A^{(M)}$  is different from  $q$  which describes the modulation of waves in a superlattice.

<sup>14</sup>We have estimated the sound velocities in the Fibonacci superlattice according to  $v^2 = (\mu^A \tau + \mu^B)/(\rho^A \tau + \rho^B)$ , which yields  $v_T = 3.51 \times 10^5$  cm/sec and  $v_L = 4.97 \times 10^5$  cm/sec for propagation perpendicular to the interfaces. For numerical values of elastic constants and densities, see S. Adachi, J. Appl. Phys. **58**, R3 (1985).

<sup>15</sup>J. Sapriel, J. C. Michel, J. C. Toledano, R. Vacher, J. Kervarec, and A. Regreny, Phys. Rev. B **28**, 2007 (1983). Numerically,  $c = 3.52 \times 10^5$  cm/sec.

<sup>16</sup>M. Kohmoto, Phys. Rev. B **34**, 5043 (1986).

<sup>17</sup>S. Tamura and J. P. Wolfe, Phys. Rev. B **35**, 2528 (1987).

<sup>18</sup>The TA mode chosen for this graph is actually the slow transverse mode, which has its polarization in the (110) plane; in this geometry, the fast transverse mode is decoupled from the LA phonon.

<sup>19</sup>We have used the values  $v_T = 3.39 \times 10^5$  cm/sec and  $v_L = 6.49 \times 10^5$  cm/sec, which are derived from the slopes of the dispersion curves in  $v \rightarrow 0$  limit.